Viscoelasticity and primitive path analysis of entangled polymer liquids: From F-actin to polyethylene ⊘

Nariya Uchida; Gary S. Grest; Ralf Everaers

Check for updates

View
Online

Export
Citation

Viscoelasticity and primitive path analysis of entangled polymer liquids: From F-actin to polyethylene

Nariya Uchida[a)]
Department of Physics, Tohoku University, Sendai 980-8578, Japan

Gary S. Grest
Sandia National Laboratories, Albuquerque, New Mexico 87185, USA

Ralf Everaers
Université de Lyon, Laboratoire de Physique, École Normale Supérieure de Lyon, CNRS UMR 5672, 46 allée d'Italie, 69364 Lyon Cedex 07, France and Max-Planck-Institut für Physik komplexer Systeme, Nöthnitzer Str. 38, 01187 Dresden, Germany

We combine computer simulations and scaling arguments to develop a unified view of polymer entanglement based on the *primitive path analysis* of the microscopic topological state. Our results agree with experimentally measured plateau moduli for three different polymer classes over a wide range of reduced polymer densities: (i) semidilute theta solutions of synthetic polymers, (ii) the corresponding dense melts above the glass transition or crystallization temperature, and (iii) solutions of semiflexible (bio)polymers such as F-actin or suspensions of rodlike viruses. Together, these systems cover the entire range from loosely to tightly entangled polymers. In particular, we argue that the primitive path analysis renormalizes a loosely to a tightly entangled system and provide a new explanation of the successful Lin-Noolandi packing conjecture for polymer melts. © *2008 American Institute of Physics.* [DOI: 10.1063/1.2825597]

I. INTRODUCTION

The relation between the complex viscoelastic properties of polymer liquids and their microscopic structure and dynamics is a key issue in materials science and biophysics.[1–5] On a microscopic scale, chains can slide past each other, but their backbones cannot cross; the Brownian motion of these macromolecules is hence subject to transient topological constraints,[6] an effect which is familiar from the manipulation of knotted strings. In slowing down the chain equilibration after a deformation, these constraints or entanglements dominate the viscoelastic behavior of high molecular weight polymeric liquids. Entanglement effects are universal, i.e., one observes the same behavior for polymers with similar overall chain architecture (linear, ring, branched) independently of details of the molecular structure. Modern theories of polymer dynamics and rheology[1,2] describe the universal aspects of the viscoelastic behavior based on the idea that molecular entanglements confine individual filaments to a one-dimensional, diffusive dynamics (reptation) in tubelike regions in space. Material specific parameters are determined through comparison with the experiment. Here, we are concerned with the question, if these parameters and related experimental observables can be inferred from the molecular structure of polymeric liquids.

How strongly linear polymers entangle with each other depends on their stiffness and on the contour length density of the polymer melt or solution.[7] The microscopic structure is best discussed in terms of the Kuhn length l_K and the number density of Kuhn segments ρ_K. The Kuhn length is defined as the contour length L, where thermal fluctuations start to bend the chains and mark the crossover from rigid rod to random coil behavior. In "loosely"[8] entangled systems with $\rho_K l_K^3 < 1$, the mean-free chain length between collisions is larger than the Kuhn length, leading to a random coil behavior between entanglement points. In contrast, for $\rho_K l_K^3 \gg 1$, filaments are "tightly"[8] entangled and exhibit only small bending fluctuations between entanglement points. As a consequence, the chains in tightly entangled F-actin solutions and in loosely entangled polyethylene melts behave differently on the tube scale. The former are essentially stiff and resist macroscopic shear due to an increase of their bending energy. The latter are flexible and lose entropy when stretched locally.

The differences between these two situations become apparent when one considers the relation between the microscopic solution structure and the height of the characteristic rubberlike plateau in the shear relaxation modulus G_N^0. In Fig. 1, we show a Graessley-Edwards plot[7] of experimentally measured[9–14] dimensionless plateau moduli $G_N^0 l_K^3/k_B T$ as a function of the dimensionless number density of Kuhn segments $\rho_K l_K^3$. For comparison, the unscaled plateau moduli are shown in the inset as a function of polymer concentration. The data we have compiled represent the behavior of several prototypical classes of entangled polymers: (i) tightly entangled solutions of semiflexible biopolymers such as F-actin and suspension of fd-phages with $\rho_K l_K^3 \gtrsim 10$, $l_K \approx 10^{-6}$ m, and $G_N^0 \approx 10^{-1}$ Pa, and (ii) loosely entangled melts of commercially important, synthetic polymers with $\rho_K l_K^3 < 10$, $l_K \approx 10^{-9}$ m, and plateau moduli of the order of $G_N^0 \approx 10^6$ Pa.

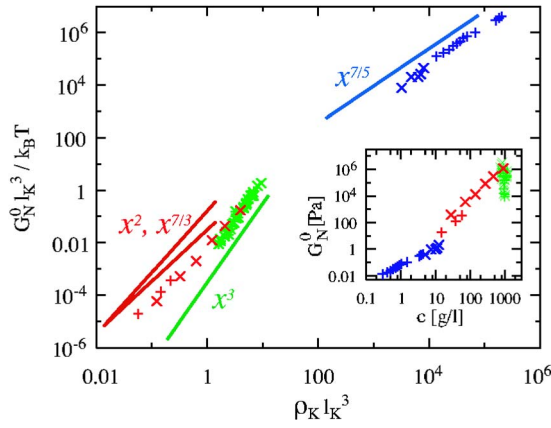a)Electronic mail: uchida@cmpt.phys.tohoku.ac.jp.

30 January 2025 15:35:47

FIG. 1. (Color online) Dimensionless plateau moduli $G_N^0 l_K^3/k_BT$ as a function of the dimensionless number density of Kuhn segments $\rho_K l_K^3$: Experimental data vs scaling predictions. Symbols indicate experimental data for (i) tightly entangled F-actin (blue +) (Ref. 9) and fd-phage (blue ×) (Ref. 10) solutions, (ii) various loosely entangled polydiene, polyolefine, and polyacrylate melts (green ×) (Refs. 11 and 12), and loosely entangled theta-solutions of polystyrene (red +) (Ref. 13) and polybutadiene(red ×) (Ref. 14). Lines represent theoretically derived power laws $G_N^0 \propto (\rho_K l_K^3)^\alpha$ for tightly (Ref. 16) and loosely (Ref. 22) entangled systems.

Typical synthetic polymers are sufficiently flexible to be in the isotropic phase in the melt state with a volume fraction $\Phi = \rho_K l_K d^2 = \mathcal{O}(1)$. In contrast, tightly entangled chains have to have a sufficiently small diameter d to fulfill the Onsager criterion $\Phi(l_K/d) < 5$ for the isotropic-to-nematic transition. We note that the crossover between the two regimes in Fig. 1 is located close to the threshold for the isotropic-nematic transition in dense polymer melts.[15] Furthermore, Fig. 1 contains data for (iii) loosely entangled semidilute solutions of synthetic polymers in the so-called theta solvents. While these systems are supposed to preserve the chain conformational statistics from the undiluted melt, the observed reduced plateau moduli are larger than those for dense systems and exhibit a qualitatively different density dependence.

For tightly entangled systems, the relation between the entanglement density ρ_e and $\rho_K l_K^3$ was determined by Semenov[16] from a geometrical argument: the area swept out via transverse fluctuations by a filament between two entanglement points is on average traversed by one other filament serving as an obstacle. In loosely entangled systems, it is impossible to determine ρ_e by scaling arguments alone.[16,23] A promising tool to solve this problem from first principles is the primitive path analysis (PPA).[12,24–28] Primitive paths were originally introduced in a thought experiment to determine the tubes confining individual polymers in an entangled polymer melt or network. The idea is to identify the random walklike tube axis with the shortest ("primitive") paths between the end points of the original chains into which the chain contours can be contracted without crossing each other.[29,30] As we have shown,[12,24] the numerical implementation of this idea allows us to make quantitative predictions of melt viscoelastic properties on the basis of a topological analysis. Here, we (i) argue that the PPA can be understood as a way of renormalizing a loosely to a tightly entangled system, (ii) derive a modified relation between the primitive path mesh characterizing an entangled polymer liquid and its

macroscopic properties (Sec. II), (iii) apply the PPA to a much wider range of loosely and tightly entangled model polymer structures (Sec. III), (iv) validate our results by a comparison to the experimental data displayed in Fig. 1, and (v) discuss the relation between the characteristic length scales of the primitive path mesh and the packing length (Sec. IV). We conclude with a brief summary in Sec. V.

II. THEORY

The result of the PPA is a mesh of mutually entangled, piecewise straight primitive paths (see, e.g., Fig. 3 in Ref. 24). The structure can be characterized by the contour length L_{pp} the mesh size $\xi_{pp} = 1/\sqrt{\rho_{chain}L_{pp}}$, and the Kuhn length a_{pp} of the primitive paths.[12,24] Furthermore, it is useful to introduce the average contour length l_e of the primitive paths between entanglement points as well as the corresponding chain contour length L_e. On a scaling level, the latter is defined implicitly by the relation

$$l_e^2 = \langle R^2 \rangle (L_e, l_K), \tag{1}$$

where $\langle R^2 \rangle (L, l_K)$ denotes the mean-square spatial distance of two points separated by a length L along the contour. The chain and primitive path statistics agree asymptotically,[1] $\lim_{L\to\infty}\langle R^2\rangle = l_K L \equiv a_{pp}L_{pp} = \lim_{L_{pp}\to\infty}\langle R^2\rangle_{pp}$ so that the Kuhn length

$$\frac{a_{pp}}{l_K} = \frac{1}{(l_e/L_e)} \tag{2}$$

of the primitive paths increases by the inverse of the shrinking factor of the contour length. Similarly the primitive path mesh size is given by

$$\frac{\xi_{pp}}{l_K} = \frac{1}{(\rho_K l_K^3)^{1/2}(l_e/L_e)^{1/2}}. \tag{3}$$

In the following, we assume (i) that all information necessary to calculate the plateau modulus of a sample can be deduced from the primitive path mesh characterizing its microscopic topological state and (ii) that the *primitive path* structure—viscoelastic property relation—is system independent, i.e., after carrying out the PPA, it is no longer necessary to distinguish between different polymer classes. Moreover, we note that by construction, primitive path meshes resemble tightly entangled solutions of semiflexible chains and that the latter are invariant under the PPA.

Regarding the primitive path analysis as a means to renormalize a loosely to a tightly entangled system, allows us to adapt two results from the theory of tightly entangled solutions of semiflexible chains[16] to the present situation:

$$\xi_{pp}^2 = c_\xi l_e \times (l_e^3/a_{pp})^{1/2}, \tag{4}$$

$$\frac{G_N^0 l_K^3}{k_BT} = c_G \left(\frac{l_K}{\xi_{pp}}\right)^2 \frac{l_K}{l_e},$$

$$= c_G c_\xi^{2/5} (\rho_K l_K^3)^{7/5} (l_e/L_e)^{8/5}. \tag{5}$$

Equation (4) expresses the idea that the area swept out via transverse fluctuations by a primitive path between two entanglement points is on average traversed by one other primi-
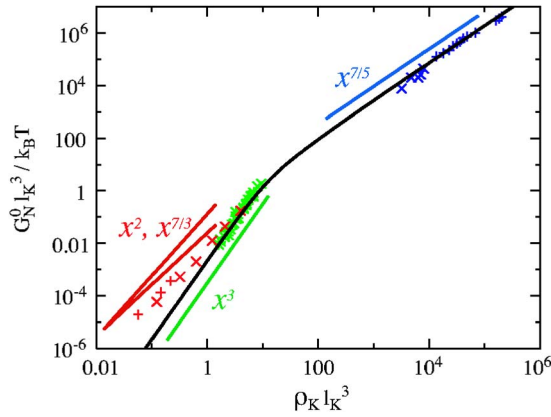
FIG. 2. (Color online) Dimensionless plateau moduli $G_N^0 l_K^3/k_B T$ as a function of the dimensionless number density of Kuhn segments $\rho_K l_K^3$: Theory vs experimental and scaling results as in Fig. 1. The black solid line indicates the combination of our Eqs. (5) and (6) with $c_\xi = 0.06$ and $c_G = 0.6$.

tive path serving as an obstacle. Equation (5) states that the plateau modulus is proportional to $k_B T$ times the density of entanglement points.

For given chain statistics, it is possible to determine l_e self-consistently from Eqs. (1)–(4). For tightly entangled systems, our approach reduces by construction to the standard results for semidilute solutions of semiflexible chains:[16,31] $a_{pp}/l_K = 1$, $\xi_{pp}/l_K = 1/(\rho_K l_K^3)^{1/2}$, $l_e/l_K \propto 1/(\rho_K l_K^3)^{2/5}$, and $G_N^0 l_K^3/(k_B T) \propto (\rho_K l_K^3)^{7/5}$. In the opposite limit, we find $a_{pp}/l_K \propto \xi_{pp}/l_K \propto 1/(\rho_K l_K^3)$ and $G_N^0 l_K^3/(k_B T) \propto (\rho_K l_K^3)^3$, i.e., we have presented a *derivation* of the Lin-Noolandi conjecture.[19,20] In the general case of solutions, where the individual polymers exhibit wormlike chain statistics on all length scales, a reasonable approximation (indicated by solid lines in all figures) is given by

$$\frac{l_e}{L_e} \approx \left(1 + \frac{L_e}{l_K}\right)^{-1/2}, \tag{6}$$

$$\frac{L_e}{l_K} \approx \left(\frac{1}{c_\xi (\rho_K l_K^3)}\right)^{2/5} + \left(\frac{1}{c_\xi (\rho_K l_K^3)}\right)^2. \tag{7}$$

By inserting Eqs. (6) and (7) into Eqs. (2), (3), and (5), we thus arrive at a prediction for the dependence of the properties of the primitive path mesh on the dimensionless Kuhn length density $\rho_K l_K^3$ of the original polymer melt or solution.

Choosing $c_\xi = 0.06$ and $c_G = 0.6$, we find excellent agreement between our theory and the experimental data for tightly entangled solutions and loosely entangled dense melts (Fig. 2). However, the Lin-Noolandi conjecture (and hence also our ansatz) fail for loosely entangled theta solutions which seem to be better described by the theory of Colby and Rubinstein.[21,22] An important oversimplification was recently pointed out by Milner:[23] by accounting only for the *mean* segment density, one implicitly treats the solvent as providing a "coating" which increases the effective chain diameter to $d/\sqrt{\Phi}$. As consequence, one neglects the increased probability of entanglement formation between closely approaching chain sections.

III. PRIMITIVE PATH ANALYSIS

Are these effects preserved in an explicit primitive path analysis? To answer this question, we have generated and analyzed model polymer liquids corresponding to the experimental data: (i) tightly entangled solutions of zero-diameter wormlike chains (WLCs) with $10 < \rho_K l_K^3 < 10^5$, (ii) dense melts of flexible bead-spring chains with $\Phi = O(1)$ and $1 < \rho_K l_K^3 < 40$, and (iii) model theta solutions generated by eliminating a fraction $0.1 < \Phi < 0.925$ of the chains from equilibrated[32] conformations of dense bead-spring chain melts.

A. Bead-spring polymer solutions and melts

For the loosely entangled regime, we used the model and procedure described in Refs. 12 and 24. Monomers are modeled as spheres of diameter σ interacting through a purely repulsive 6-12 Lennard-Jones (LJ) potential, which is short ranged and purely repulsive. The polymers are formed by connecting beads via finitely extensible nonlinear elastic springs. The average bond length is $b = 0.97\sigma$. The parameter choice ensures that two chains cannot cross each other in dynamic simulations. Monodisperse polymer melts of $M = 80-500$ chains of length $50 \leq N \leq 700$ at a bead density of $\rho = 0.85\sigma^{-3}$ are studied. By introducing a small intrinsic bond bending potential, l_k is varied between 1.82σ and 3.34σ, for details see Ref. 32. For dense systems, we extended the data from Ref. 24 by one additional data point for larger intrinsic bending stiffness close to the isotropic nematic transition. Furthermore, we equilibrated two Kremer-Grest theta solutions $M = 200$ chains of length $N = 700$ at bead densities of $\rho = 0.25\sigma^{-3}$ and $\rho = 0.4\sigma^{-3}$. In this case, the LJ cutoff is set to $r_c = 2.5\sigma$ and simulations are carried out at $k_B T = 3.0\epsilon_{LJ}$. To obtain a large number of model theta solutions whose intra- and interchain correlations are *identical* to those of the dense systems, we randomly eliminate a fraction $0.1 < \Phi < 0.925$ of the chains from equilibrated[32] conformations of dense bead-spring chain melts with $N = 7000$. The PPA is implemented into a standard molecular dynamics code:[12,24] Chain ends are fixed in space, intrachain excluded volume as well as bending interactions are disabled, and chain contraction is induced by cooling the system toward $T = 0$.

B. Entangled solutions of zero-diameter WLCs

Data covering the crossover to the tightly entangled regime were mainly obtained using Monte Carlo techniques. We have generated and analyzed semidilute solutions of infinitely thin wormlike chains with $1 \leq \rho_K l_K^3 \leq 10^5$. Bending of the chain was penalized by the Hamiltonian $H/k_B T = -(l_p/b) \sum_{i=1}^{L-1} \mathbf{u}_i \cdot \mathbf{u}_{i+1}$, where b denotes the segment length, $l_p = \kappa/k_B T$ is the persistence length of the continuum wormlike chain with the bending modulus κ, and $\mathbf{u}_i$ the unit vector along the axis of the ith cylinder. Chains of this type have a Kuhn length of $l_K^{(0)}/b = 2/(1 + b/l_P - \coth l_P/b) - 1$ and can be efficiently generated by simple sampling. In the absence of interchain correlations for zero chain diameter, fully
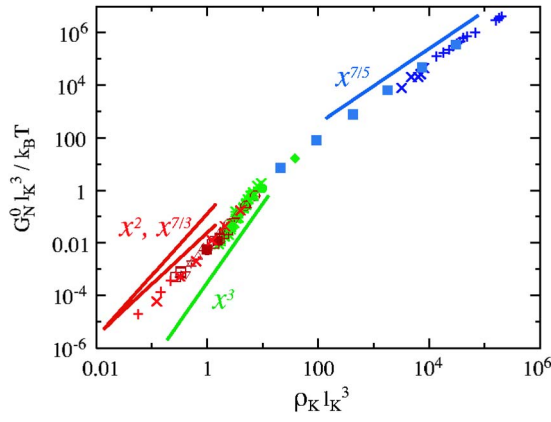
FIG. 3. (Color online) Dimensionless plateau moduli $G_N^0 l_K^3 / k_B T$ as a function of the dimensionless number density of Kuhn segments $\rho_K l_K^3$: PPA vs experimental and scaling results as in Fig. 1. Additional symbols indicate PPA results for (i) tightly entangled, zero-diameter wormlike chains (blue □), (ii) Kremer-Grest melts and theta solutions (red and green filled symbols) for bead-spring polymers with intrinsic stiffness □<△<▽<○<◇. Furthermore, we have included PPA results for model theta solutions (open red symbols) created by eliminating chains from the corresponding melts.

equilibrated semidilute solutions are obtained by placing N randomly generated chains into a cubic box of size L_{box}^3 with periodic boundary conditions. As a general rule, the chains were chosen to be long enough to be multiply entangled and the linear dimension of the simulation box exceeds the typical chain extensions. For the PPA, we used a brownian dynamics/force-biased Monte Carlo simulation code for entangled wormlike chains, which rejects moves leading to chain crossing. Starting from the solution conformations, the positions of the chain ends are fixed. Chain contraction is induced by setting chain stiffness as well as the equilibrium extension of the segments to zero and reducing the temperature.

C. Estimating plateau moduli from the PPA

Following again Refs. 12 and 24, we measure mean-square internal distances $\langle r_{pp}^2(|i-j|\rangle$ as a function of chemical distance $|i-j|$ to determine the Kuhn length a_{pp} and the contour length L_{pp} of the primitive paths.

For flexible polymers, the standard relation between the plateau modulus and the length scales characterizing the primitive path mesh is[1]

$$\frac{G_N^0 l_K^3}{k_B T} \propto (\rho_K l_K^3) \left(\frac{l_k}{a_{pp}} \right)^2. \tag{8}$$

Here, we have instead used Eq. (5) which can be written as

$$\frac{G_N^0 l_K^3}{k_B T} = c_G c_\xi^{2/5} (\rho_K l_K^3)^{7/5} \left(\frac{l_k}{a_{pp}} \right)^{8/5}. \tag{9}$$

Equations (8) and (9) are equivalent, if $a_{pp}/l_K \propto \xi_{pp}/l_K \propto 1/(\rho_K l_K^3)$, i.e., for the dense, loosely entangled melts where Eq. (8) was used in Ref. PPA. However, Eq. (8) clearly fails in the tightly entangled regime and we also found less good agreement with experimental data for estimates of plateau moduli for theta solutions (data not shown).
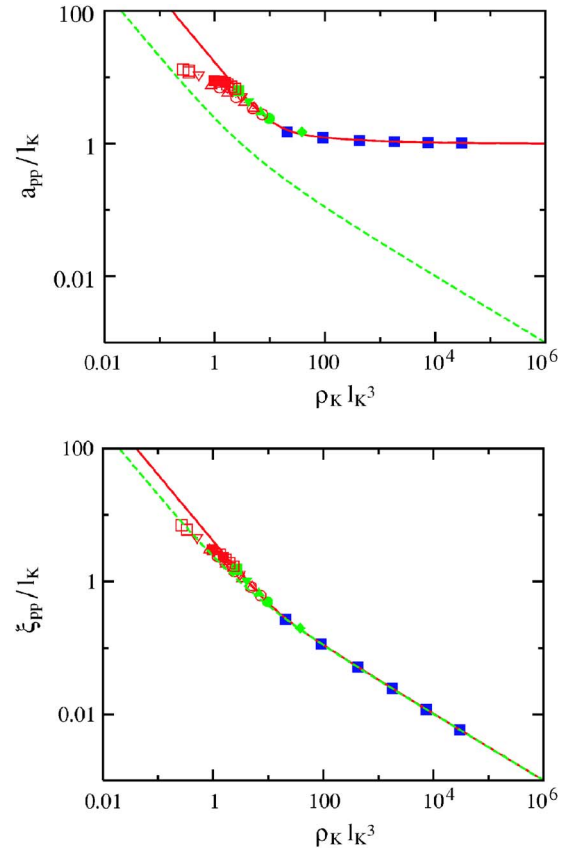

FIG. 4. (Color online) Kuhn length a_{pp}/l_K and mesh size ξ_{pp}/l_K for the primitive path mesh as a function of the dimensionless number density of Kuhn segments $\rho_K l_K^3$. The solid lines indicate the combination of Eq. (6) with Eqs. (2) and (3), respectively, with $c_\xi = 0.06$ and $c_G = 0.6$. The dashed line represents the packing length Eq. (12). Symbols indicate PPA results for zero-diameter wormlike chains (blue), dense bead-spring melts (green), and model theta solutions (red).

IV. RESULTS AND DISCUSSION

In Fig. 3, we show our PPA results for the plateau moduli in comparison with the experimental data. The PPA identifies the location of the crossovers from the theta solution to the dense melts and from the loosely to the tightly entangled regime with no adjustable parameters. In particular, we obtain *quantitative* agreement with the experimentally measured moduli by adjusting a *single* parameter (equal to $c_G c_\xi^{2/5} = 0.2$) for the strength of the elastic response. Before we take a closer look at the results for loosely entangled theta solutions, we discuss the microscopic length scales characterizing the primitive path mesh.

In Fig. 4, we show the Kuhn lengths a_{pp} and mesh sizes ξ_{pp} which we extracted for the various model systems. As for the predicted moduli, the results for tightly entangled WLC solutions and for dense melts of flexible bead-spring chains are in excellent agreement with our theoretical results. Note that there are no adjustable parameters in addition to the values of $c_\xi = 0.06$ and $c_G = 0.6$ derived from the above experimentally measured plateau moduli.

Interestingly, the primitive path (PP) mesh size ξ_{pp} is essentially given by the packing length p. This length scale was introduced[33] as the characteristic spatial distance where different polymers start to interpenetrate, i.e., the length scale

where the intra- and interchain monomer pair correlation functions coincide: $g_{intra}(p) \equiv g_{inter}(p)$. In the systems we investigate that interchain correlations are small, so that we use $g_{inter}(p) \equiv 1$ or $\partial L(p, l_K)/\partial p \equiv p^2 \rho_K l_K$ to calculate the packing length. Using

$$\langle R^2 \rangle (L, l_K) \approx L^2/(1 + L/l_K), \tag{10}$$

$$L(r, l_K) \approx r(1 + r/l_K), \tag{11}$$

the result is

$$\frac{p}{l_K} \approx \frac{1 + \sqrt{1 + (\rho_K l_K^3)}}{(\rho_K l_K^3)}. \tag{12}$$

The limiting cases are again simple to understand. For $p \gg l_K$, the chain contour length L contained in a volume p^3 is much longer than the Kuhn length l_K. The chains follow a random walk statistics with $\langle R^2 \rangle = l_K L$. In this case, the packing length is given by $p = (\rho_{chain} \langle R^2 \rangle)^{-1}$,[33] and with $p/l_K \propto a_{pp}/l_K \propto \xi_{pp}/l_K \propto 1/(\rho_K l_K^3)$, the packing length turns out to be the only relevant length scale in loosely entangled systems.[11,24] In the opposite limit, when $p \ll l_K$, the single chain statistics corresponds to a rigid rod with $\langle R^2 \rangle = L^2$. In this case, $p = (\rho_{chain} \langle R^2 \rangle^{1/2})^{-1/2} = 1/(\rho_K l_K)^{1/2}$, i.e., p is identical to the mesh size of the solution as well as the primitive path mesh. In contrast to the previous case, the Kuhn length $a_{pp} = l_K$ of both chains and primitive paths remains as a second, independent length scale.

As a last point, we come back to the case of loosely entangled (model) theta solutions. Both experimental and PPA results for plateau moduli show clear deviations from our theory (respectively the packing conjecture) $G_N^0 l_K^3/(k_B T) \propto (\rho_K l_K^3)^3$ and the corresponding extrapolation of the behavior of loosely entangled dense melts (Fig. 3). Qualitatively, sufficiently dilute systems behave in accordance with a power law $G_N^0 l_K^3/(k_B T) \propto (\rho_K l_K^3)^\alpha$, where the exponent α is in the range of the predictions[22] of the binary contact model ($\alpha = 2$) (Refs. 17 and 18) and the Colby-Rubinstein model ($\alpha = 7/3$).[21,23] However, for the relatively dense model theta solutions which we analyzed using the PPA, we see no evidence for immediate departures from the packing line of the form $G_N^0(\Phi) = G_N^0(\Phi = 1)\Phi^\alpha$, i.e., for a family of curves with identical slope but different prefactors essentially determined by the plateau moduli of the undiluted melt. Rather, data obtained for model theta solutions map fairly well onto each other and continue to map onto the melt results as long as $\rho_K l_K^3 > 1$. Deviations only occur for lower concentrations.

The comparison can be extended to the length scales characterizing the primitive path meshes. Inserting the predictions for $N_e \equiv L_e/l_K$ of the binary contact and the Colby-Rubinstein model into Eqs. (2) and (3) (which follow directly from the definitions and hold independently of the applicability of the Semenov theory to the primitive path mesh) yields $a_{pp}/l_K \propto (\rho_K l_K^3)^{-1/2}$, $\xi_{pp}/l_K \propto (\rho_K l_K^3)^{-3/4}$ and $a_{pp}/l_K \propto (\rho_K l_K^3)^{-2/3}$, $\xi_{pp}/l_K \propto (\rho_K l_K^3)^{-5/6}$, respectively. In particular, one obtains for the ratio $a_{pp}/\xi_{pp} \propto (\rho_K l_K^3)^{1/4}$ and $a_{pp}/\xi_{pp} \propto (\rho_K l_K^3)^{1/6}$, respectively. Thus, in the limit in question where $(\rho_K l_K^3)$ can become arbitrarily small, these models predict that the area a_{pp}^2 mapped out by two subsequent Kuhn

segments of a primitive path is on average traversed by *less than one* other primitive path which could serve as an obstacle. The results of the actual PPA shown in Fig. 4 allow no definite conclusion. Naive extrapolation would indeed lead to $a_{pp} < \xi_{pp}$ in the limit $(\rho_K l_K^3) \to 0$. However, we note that we have never observed this inversion. Interestingly, the deviations from our theory occur once p exceeds l_K and the results of the explicit PPA for theta-solutions are compatible with a crossover to a pure packing scenario with $p/l_K = a_{pp}/l_K = \xi_{pp}/l_K \propto 1/(\rho_K l_K^3)$, where the PP directions before and after an entanglement point become completely uncorrelated.

V. SUMMARY AND CONCLUSION

There is a wide spectrum of entangled polymer liquids whose single chain structure is characterized by a single microscopic length scale, the Kuhn, or persistence length. Our starting point was a compilation of experimentally measured plateau moduli for semidilute theta solutions of synthetic polymers, the corresponding dense melts above the glass transition or crystallization temperature, and solutions of semiflexible (bio)polymers such as F-actin or suspensions of rodlike viruses. Together, these systems cover the entire range from loosely to tightly entangled polymers. In this article, we have demonstrated excellent agreement between the experimentally measured plateau moduli and our results derived from a primitive path analysis[24] of corresponding model polymer liquids. This is a strong evidence supporting our working hypothesis that the PPA may be regarded as a tool to renormalize a loosely to a tightly entangled system: while the relation between the microscopic structure and the viscoelastic properties is different for the three classes of entangled polymer liquids included in the present study, these differences vanish in the course of the PPA. In particular, experimental properties can be calculated by applying relations for tightly entangled systems to the primitive path mesh *independently* of the character of the original system [note that Eq. (5) for the plateau modulus reduces to the standard expression[1] Eq. (8) in the case of loosely entangled melts; however, the latter *fails* in the tightly entangled regime]. This ansatz provided a new explanation of the Lin-Noolandi packing conjecture[19,20] and allowed us to derive simple analytical expressions for macroscopic (Fig. 1) and microscopic (Fig. 4) entanglement properties which are in excellent agreement with the experimental and simulation data over a wide range of reduced polymer densities. Future work has to show whether the Colby and Rubinstein scaling[21] in theta solutions is a cross over effect or valid asymptotically and whether it is possible to account for density fluctuations by combining the arguments and methods presented in this paper with the scaling analysis of loosely entangled solutions presented in Ref. 23. Judging from the available experimental and PPA results, this might be necessary to "disentangle" the influence of the various crossovers in the experimentally relevant parameter range.

ACKNOWLEDGMENTS

[1] M. Doi and S. F. Edwards, *The Theory of Polymer Dynamics* (Clarendon, Oxford, 1986).

[2] T. C. B. McLeish, Adv. Phys. **5**, 1379 (2002).

[3] D. Boal, *Mechanics of the Cell* (Cambridge University Press, Cambridge, 2002).

[4] J. Bent, L. R. Hutchings, R. W. Richards, T. Gough, R. Spares, P. D. Coates, I. Grillo, O. G. Harlen, D. J. Read, R. S. Graham, A. E. Likhtman, D. J. Groves, T. M. Nicholson, and T. C. B. McLeish, Science **301**, 1691 (2003).

[5] A. Bausch and K. Kroy, Nat. Phys. **2**, 231 (2006).

[6] S. F. Edwards, Proc. Phys. Soc. London **91**, 513 (1967).

[7] W. W. Graessley and S. F. Edwards, Polymer **22**, 1329 (1981).

[8] D. C. Morse, Macromolecules **31**, 7030 (1998).

[9] B. Hinner, M. Tempel, E. Sackmann, K. Kroy, and E. Frey, Phys. Rev. Lett. **81**, 2614 (1998).

[10] F. G. Schmidt, B. Hinner, E. Sackmann, and J. X. Tang, Phys. Rev. E **62**, 5509 (2000).

[11] L. J. Fetters, D. J. Lohse, D. Richter, T. A. Witten, and A. Zirkel, Macromolecules **27**, 4639 (1994).

[12] S. K. Sukumaran, G. S. Grest, K. Kremer, and R. Everaers, J. Polym. Sci., Part B: Polym. Phys. **43**, 917 (2005).

[13] T. Inoue, Y. Yamashita, and K. Osaki, Macromolecules **35**, 9169 (2002).

[14] R. Colby, L. J. Fetters, W. G. Funk, and W. W. Graessley, Macromolecules **24**, 3873 (1991).

[15] The location of the isotropic-nematic transition is given by the Onsager criterion $\rho_K l_K^2 d \approx 5$. Dense melts with polymer volume fractions $\Phi = \rho_K l_K d^2 = \mathcal{O}(1)$ are isotropic for sufficiently flexible chains with aspect ratios $l_K/d < 5$ or $\rho_K l_K^3 < 25$. In contrast, isotropic, tightly entangled solutions with $\rho_K l_K^3 \gg 1$ can only be formed by semiflexible chains with large aspect ratios $l_K/d \gg (\rho_K l_K^3)^{1/2}$.

[16] A. N. Semenov, J. Chem. Soc., Faraday Trans. **82**, 317 (1986).

[17] P. G. de Gennes, J. Phys. (France) Lett. **35**, L133 (1974).

[18] F. Brochard and P. G. de Gennes, Macromolecules **10**, 1157 (1977).

[19] Y.-H. Lin, Macromolecules **20**, 3080 (1987).

[20] T. A. Kavassalis and J. Noolandi, Phys. Rev. Lett. **59**, 2674 (1987).

[21] R. H. Colby and M. Rubinstein, Macromolecules **23**, 2753 (1990).

[22] R. H. Colby, M. Rubinstein, and J. L. Viovy, Macromolecules **25**, 996 (1992).

[23] S. Milner, Macromolecules **38**, 4929 (2005).

[24] R. Everaers, S. K. Sukumaran, G. S. Grest, C. Svaneborg, A. Sivasubramanian, and K. Kremer, Science **303**, 823 (2004).

[25] M. Kröger, Comput. Phys. Commun. **168**, 209 (2005).

[26] S. Shanbhag and R. G. Larson, Phys. Rev. Lett. **94**, 076001 (2005).

[27] Q. Zhou and R. Larson, Macromolecules **38**, 5761 (2005).

[28] C. Tzoumanekas and D. Theodorou, Macromolecules **39**, 4592 (2006).

[29] S. F. Edwards, Br. Polym. J. **9**, 140 (1977).

[30] M. Rubinstein and E. Helfand, J. Chem. Phys. **82**, 2477 (1985).

[31] D. C. Morse, Phys. Rev. E **63**, 031502 (2001).

[32] R. Auhl, R. Everaers, G. S. Grest, K. Kremer, and S. J. Plimpton, J. Chem. Phys. **119**, 12718 (2003).

[33] T. A. Witten, S. T. Milner, and Z.-G. Wang, in *Multiphase Macromolecular Systems*, edited by B. M. Culbertson (Plenum, New York, 1989).